Effect of Phosphorus on the Hardness Temperature Resistance of Nanostructured Ni-W Electrodeposited Coatings

M J.L. Gines, M. J. Loureiro and F.J. Williams*
REDE-AR, SIDERCA-TENARIS
Department of Surface Chemistry and Coatings
Buenos Aires, Argentina

The development of electrodeposited coatings with enhanced properties is nowadays focused on nanotechnology. More specifically, the development of temperature-resistant hard coatings for a wide variety of applications is gaining attention. Hard chromium coatings electrodeposited from hexavalent plating baths are widely used for improving hardness, wear resistance and the decorative appearance of engineering tools and components despite the serious health and environmental problems they cause. Therefore, researchers have been looking for adequate replacements of Cr-based coatings. Nanostructured Ni-W coatings are one of the potential replacements that have been extensively studied. In this work, we investigated the mechanical properties/temperature dependence of electrodeposited Ni-W and Ni-W-P coatings. Changes in composition were controlled by changing the phosphorus concentration in the plating bath. The presence of phosphorus improves the mechanical property temperature resistance of the electrodeposited Ni-W coatings.

Keywords: *nanostructured coatings, nanotechnology, nickel-tungsten, nickel-tungsten-phosphorus, chromium replacement coatings, temperature resistance*

Introduction

Hard chromium coatings based on hexavalent chromium plating are widely used for improving the hardness, wear, erosion resistance and decorative appearance of engineering tools and components,[1-5] despite the potentially serious health and environmental problems involved in their process chemistry.[6] Therefore, there has been considerable effort to find adequate replacements of chromium and Cr-based coatings to eliminate the use of hexavalent chromium.

Alternatives that have already been investigated include cobalt- and nickel-based coatings.[7] Nickel-tungsten (Ni-W) coatings are one of the replacements that have been extensively analyzed, because they have a unique combination of tribological, mechanical, magnetic, electrical and electro-erosion properties.[7-9] One of the drawbacks that Ni-W coatings have for some tooling application is that the microhardness decreases when heating at temperatures used in some tooling applications. It is therefore desirable to improve this behavior.

The addition of small amounts of tungsten (3.5 at%) to electroless Ni-P (82.0 at% Ni - 14.5 at% P) coatings enhance the thermal stability and mechanical properties for the ternary Ni-P-W systems.[10] Ni-P-W multilayered alloy coatings with layer thicknesses ranging from 8 to 4200 nm obtained by pulse plating show an increase in hardness in the 500 to 600°C range, which decreases as the annealing temperature increases.[11,12] Given that adding small amounts of phosphorous improves the hardness temperature resistance of Cr-based coatings,[13] it is worthwhile to study its effect on Ni-W coatings.

In this work we electrodeposited uniform Ni-W-P coatings using NaH_2PO_2 as a source of phosphorus. Coatings with grain sizes in the nanometer range were obtained employing bipolar pulsed current (BPP).[14] In this method, a reverse pulse selectively removes atoms with the highest oxidation potential from the deposit, inhibiting grain growth during electrodeposition.[14,15] Therefore changes in coating composition and hence in average grain sizes were controlled by changes in the current density of reverse pulses and changes in the phosphorus concentration in the plating bath. The effect of temperature on the coating microhardness was analyzed as a function of phosphorus content. We found that adding small quantities of phosphorus significantly increased the microhardness

* *Corresponding author:*
Dr. Marcelo Gines
SIDERCA-TENARIS-CINI
Dr. Simini 250
B2804MHA, Campana, Argentina
Phone: 54 3489 433100 Ext 34521
Fax: 54 3489 427928
E-mail: mgines@tenaris.com

temperature resistance of Ni-W coatings. Furthermore, improved Ni-W-P coatings exhibited better microhardness temperature resistance than hard chromium coatings.

Experimental procedures

Electrodeposition and thermal treatment

Ni-W and Ni-W-P were deposited on steel plates using the electroplating bath shown in Table 1 with $NaH_2PO_2 \cdot H_2O$ as the source of phosphorus. Electrodeposition was carried out in an 800 mL (0.211 gal) jacketed glass cell containing the electroplating bath, which was agitated using a magnetic stirrer and heated to a temperature of 75°C (167°F) using a thermostatic heating bath. The cathode consisted of carbon steel with an exposed surface area of 15 cm^2 (2.34 in^2), and was separated by about 3.5 cm (1.38 in) from a platinum mesh anode.

Prior to electrodeposition, the steel cathodes were thoroughly cleaned using the following procedure: (1) ultrasound in a 20% aqueous solution of a proprietary cleaner, (2) electrolytic treatment (0.3 A/cm^2 (1.93 A/in^2) for 2 min) using a 23.2 g/L (3.10 oz/gal) aqueous solution of NaOH and (3) immersion in a 10% aqueous solution of H_2SO_4 (10%) for 15 sec.

The cathodic pulses used to deposit Ni-W-P coatings were run for 20 msec at a current density of 0.2 A/cm^2 (1.29 A/in^2) while the anodic pulses were run for 3 msec at a current density of 0.05 A/cm^2 (0.32 A/in^2). Pulses for Ni-W-P deposition were similar but the anodic pulses were maintained at 0.05 A/cm^2 (0.32 A/in^2).

Characterization techniques

The surface morphology and polished cross-sections of the as-deposited and annealed samples were characterized with a Philips XL-30 scanning electron microscope (SEM). Semi-quantitative chemical composition was determined by calibrated energy dispersive x-ray spectroscopy (EDS). Thicknesses were directly measured on metallurgically-prepared cross-sections of the electrodeposits using SEM images.

X-ray diffraction (XRD) was employed to determine the coating microstructure. XRD patterns were collected at room temperature with a Philips X'Pert diffractometer using CuKα radiation (λ = 1.5405 Å). From the data obtained, crystallite sizes were determined using the width of the Ni(111) peak, after correcting for line-broadening.[16,17]

Table 1

Bath composition used to electrochemically deposit Ni-W-P

Bath constituent	Concentration [M]	Function
$NiSO_4 \cdot 6H_2O$	0.06	Source of Ni
$Na_2WO_4 \cdot 2H_2O$	0.14	Source of W
$NaH_2PO_2 \cdot H_2O$	0.0024 - 0.472	Source of P
$Na_3C_4H_5O_7 \cdot 2H_2O$	0.5	Ni and W complexer
NH_4Cl	0.5	Increases current efficiency
NH_4OH	As needed	pH stabilizer

Microhardness tests were conducted with a LECO microindenter model LM 247AT on both as-received and metallurgically-prepared cross-sections of the electrodeposits, using a Vickers indenter with 10 and 25 g load, respectively. Ten measurements were made for each load and the average was reported.

Results and discussion

Characterization of as-deposited Ni-W and Ni-W-P coatings

Table 2 shows the composition of Ni-W-P coatings as a function of NaH_2PO_2 added to the bath. The tungsten content diminished as the reverse current density increased, due to the preferential removal of elements with higher oxidation potential during the flow of a reverse current.[15]

Table 2

Average compositions of deposited Ni-W-P coatings

Sodium Hypophosphite in Bath, g/L	P content, at%	W content, at%	Ni content, at %
0.0	0.0	28.2	71.8
0.25	4.5	25.3	70.1
0.50	7.4	23.4	68.7
1.0	13.4	17.8	68.8
2.0	29.4	2.7	68.0
5.0	32.3	1.1	66.6

Semiquantitative chemical composition showed that the amount of phosphorus deposited could be controlled by adjusting the NaH_2PO_2 concentration in the bath. Similar results were found by Ahmad, *et al.*,[18] who showed that for a low concentration of 0.99 g/L (0.13 oz/gal), slight changes in concentration resulted in sharp changes in the phosphorus content of deposited alloys whereas greater concentration saturated the phosphorus content in the coating. Table 2 shows that as the amount of deposited phosphorus increased, the amount of nickel decreased by 7%, whereas the amount of tungsten deposited decreased by 96%. Concentrations of phosphorus lower than 0.5 g/L (0.07 oz/gal) resulted in coatings with similar Ni-W ratios.

Figure 1 shows SEM micrographs of Ni-W-P coatings as a function of increasing phosphorus concentration. It is clear that phosphorus caused differences in morphology with differences in composition. The spherical clusters observed in Ni-W appeared also in the Ni-W-P coatings. The clusters grew with increasing NaH_2PO_2 concentration in the bath up to 0.5 g/L (0.07 oz/gal). The cluster size then began to decrease with higher concentrations. It is also important to mention that increasing the phosphorus content in the bath caused a thinning of all coatings, as a result of a reduced rate of electrodeposition, in agreement with previous studies.[13,18]

Figure 2 shows the XRD pattern of Ni-W coatings as a function of phosphorus concentration. The XRD of Ni (not shown here) revealed clearly that the addition of tungsten caused a broadening of the nickel peaks and a shift to lower angles. This is attributed to the reduction of average crystallite size and crystallinity together with the increase of tungsten as an alloying element. This behavior agrees with the results of several other authors.[15,19-21] The Ni-W-P coatings prepared under the same conditions were also amorphous. The XRD patterns show that the width of the diffraction peaks increased with higher phosphorus and lower tungsten content, which means that crystallinity decreased with increasing phosphorus content. In agreement with our findings, Ahmad, *et al.*[18] reported that Ni-W coatings became completely amorphous when the phosphorus content increased beyond ~5 at%.

Figure 3 shows the average grain size calculated from the XRD pattern shown in Fig. 2 as a function of phosphorus concentration in the bath. The crystallite size in the Ni-W-P coatings decreased with increasing phosphorus content in the bath, which also resulted in a decrease in the tungsten content (Fig. 3).

Figure 4 shows the microhardness of the Ni-W-P coatings as a function of phosphorus content in the plating bath. Hardness values ranged from 506 kgf/mm^2 for the lowest tungsten content (1.1 at% W) and highest phosphorus content (32.3 at% P) to 686 kgf/mm^2 for the highest tungsten content (28.2 at% W) and the lowest phosphorus content (0 at% P). In agreement with other authors, we found that the Ni-W coatings without phosphorus became harder with higher tungsten content.[8,15,20,21] From these results, it is clear that phosphorus regulated the tungsten content in Ni-W coatings. Increasing the phosphorus content resulted in lowering the tungsten content (from 28.2 to 1.1 at% W), decreasing grain size (from 6.0 to 1.0 nm), and decreasing the coating microhardness (from 686 to 506 kgf/mm^2). The dependence of microhardness with grain size for Ni-W coatings in the absence and presence of phosphorus is discussed below.

Figure 5 shows the relationship between the inverse root of the apparent grain size and the microhardness of all as-deposited Ni-W and Ni-W-P coatings. The graph shows that the microhardness increased proportionally to the inverse of the square root of the grain size with increasing grain size up to a size of ~6 nm and then decreased proportionally with the square root of the grain size. The observed behavior at large grain sizes ($d > 6$ nm) followed the Hall-Petch relationship as expected.[22,23] However, for small grain sizes an inverse Hall-Petch relationship was observed, in agreement with Ni-W and Ni-W-P materials.[18,19]

Characterization of the annealed Ni-W and Ni-W-P coatings

The XRD patterns as a function of the concentration of NaH_2PO_2 in the plating bath are depicted in Fig. 6. As the annealing temperature increased, the crystallinity of the coating material increased and new phases appeared. Furthermore, the average crystallite sizes increased with increasing annealing temperature for all Ni-W-P samples.

Figure 6 shows that the width of the XRD peaks decreased with increasing annealing temperature and with decreasing phosphorus content. All samples annealed appeared to be amorphous for annealing temperatures below 300°C (572°F). Also, all samples annealed at higher temperatures, except for the one prepared with 1.0 g/L (0.134 oz/gal) NaH_2PO_2, were clearly crystalline.

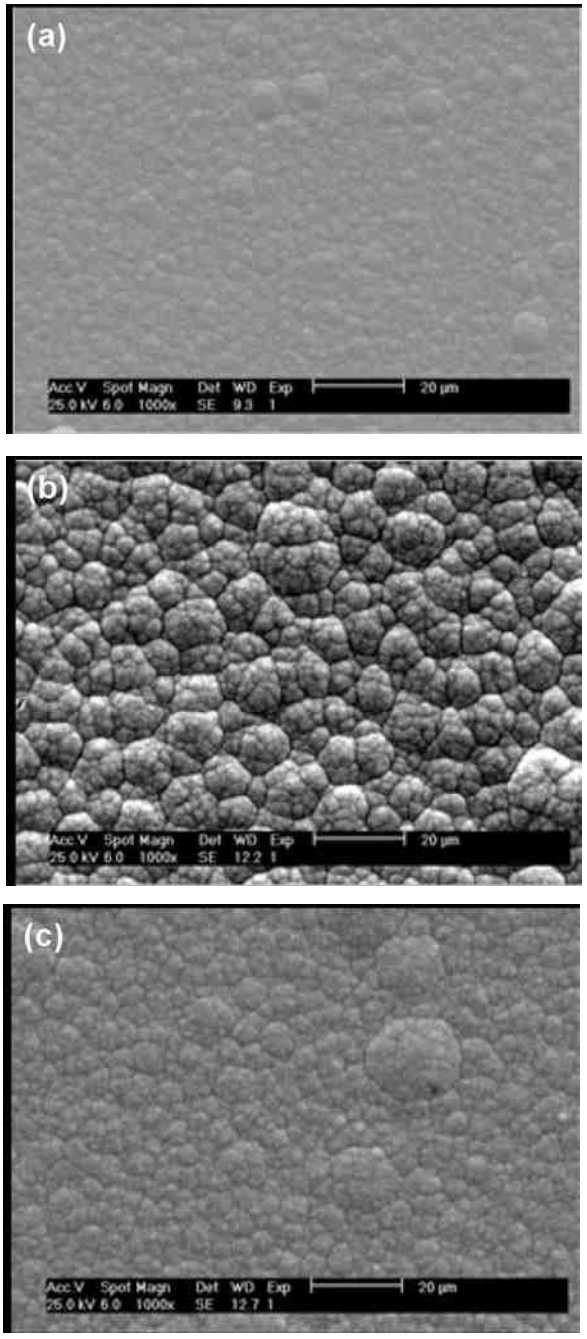

Figure 1—*Surface SEM images of Ni-W-P coatings prepared with a) 0.0 g/L, b) 1.0 g/L and c) 2.0 g/L of sodium hypophosphite.*

Annealing at temperatures above 600°C (1112°F) caused the formation of new phases in the Ni-W-P coatings. Ni_3P peaks began to appear at 600°C (1112°F) and became sharper with increasing temperature. Several oxide phases were also detected with XRD. Nickel oxide (NiO) peaks began to appear at 600°C (1112°F), and sharp $NiWO_4$ and WO_3 peaks appeared at 800°C (1472°F). In addition, it is important to note that, as previously observed in Ni-P and Ni-P-W coatings, the temperature of crystallization of the electrodeposited coatings increased with increasing phosphorus content. Higher temperatures were needed to crystallize Ni-W-P as the phosphorus content increased. The same behavior has been observed for Cr-C-P coatings.[13]

Figure 7 shows the dependence of the average crystallite size of the Ni-W-P coatings as a function of annealing temperature. Clearly grain growth occurred during heat treatment, with grain sizes of Ni-W-P larger than those of Ni-W for temperatures above 300°C (572°F).

Figure 8 shows the effect of annealing temperature on the microhardness (measured at room temperature) of Ni-W and Ni-W-P coatings. The addition of phosphorus to the Ni-W electroplating bath and the consequent co-deposition of Ni-W-P had an important effect on the microhardness of the material. Even though at room temperature, the hardness of Ni-W-P was lower than that of Ni-W, we found that at higher temperatures the opposite was true. Furthermore, it should be noted that annealed Ni-W and Ni-W-P coatings reached higher hardness values than those obtained by conventional hard chromium coatings (full circles in Fig. 8) at annealing temperatures greater than 300°C (572°F).[13]

Why does the incorporation of phosphorus into the Ni-W coatings result in higher hardness with annealing temperatures? The increase in microhardness with increasing annealing temperature should be attributed to the increasing crystallization of materials, resulting in the formation of a nanocrystalline alloy. The increased precipitation of the hard intermetallic Ni_3P within grain boundaries of the Ni-W matrix avoided deformation and thus increased hardness. Since the amount of Ni_3P present increased with increasing annealing temperature, increased hardness could be attributed to increasing formation of this compound. This agrees with the behavior of electrodeposited multilayered Ni-W-P systems.[12]

The decrease in hardness when annealing to 800°C (1472°F) is attributable to the significant increase in grain size, which is explained by the Hall-Petch relationship.[23] However, it is worth mentioning that since the grain size of Ni-W-P coatings did not increase significantly, its hardness only decreased slightly. The hardness of annealed Ni-W-P coatings with low phosphorus content (4.5 and 7.4 at% P) did not show values below 856 kgf/mm^2, which are close to the highest values reached by the Ni-W coatings. Thus, although the hardness of Ni-W-P began to decay above 600°C (1112°F), the Ni-W-P coatings were still superior to Ni-W with regard to the hardness dependence with annealing temperature.

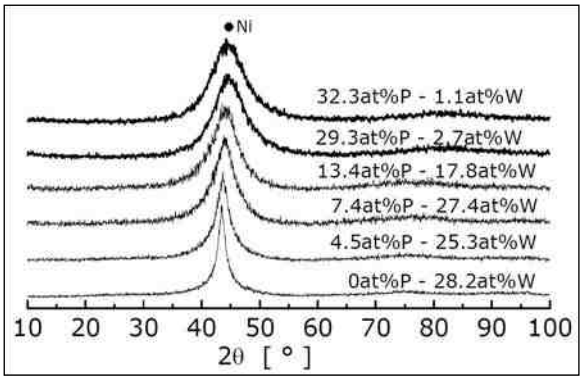

Figure 2—*X-ray diffraction patterns obtained from as-deposited Ni-W-P coatings prepared as a function of phosphorus content.*

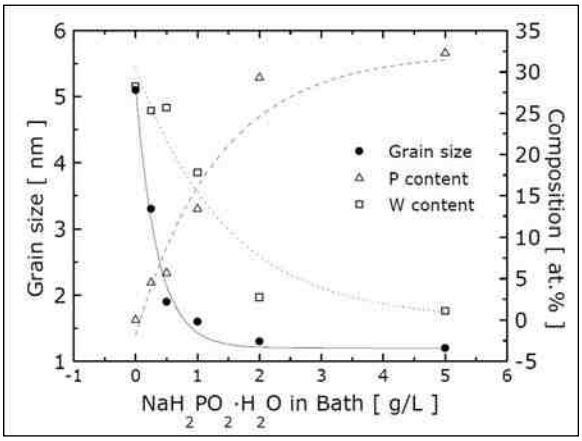

Figure 3—*Effect of composition on crystallite size of Ni-W-P.*

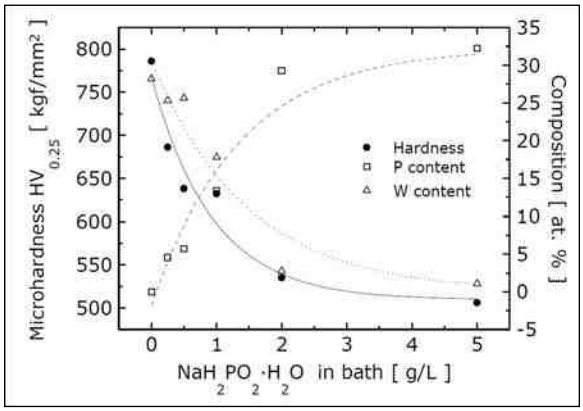

Figure 4—*Effect of $NaH_2PO_2{\cdot}H_2O$ concentration in plating bath on composition and microhardness of Ni-W-P coatings.*

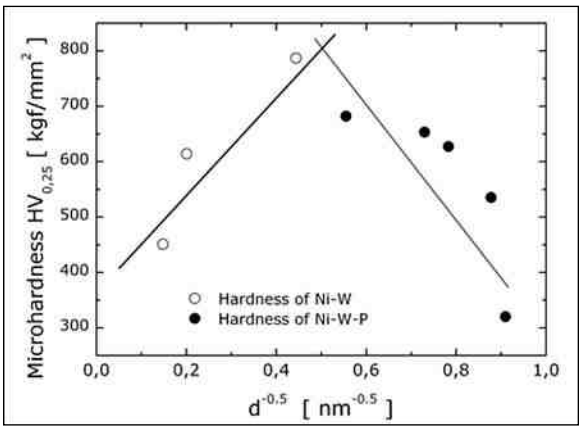

Figure 5—*Relationship between apparent crystallite size and microhardness of as-deposited Ni-W-P coatings.*

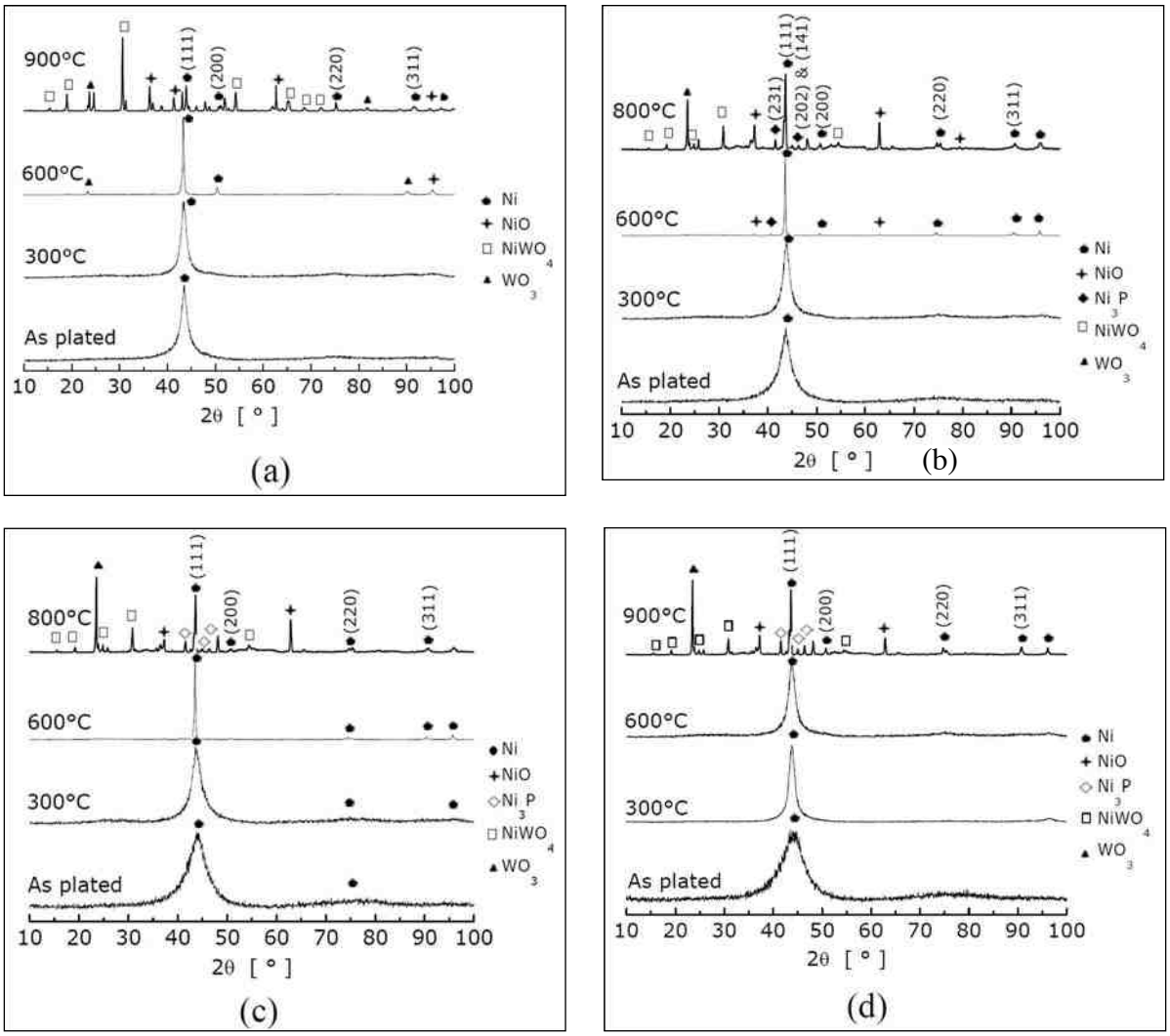

Figure 6—*X-ray diffraction patterns for as-deposited and annealed samples of Ni-W-P coatings prepared with a) 0.0 g/L, b) 0.25 g/L, c) 0.5 g/L, and d) 1.0 g/L of $NaH_2PO_2 \cdot H_2O$.*

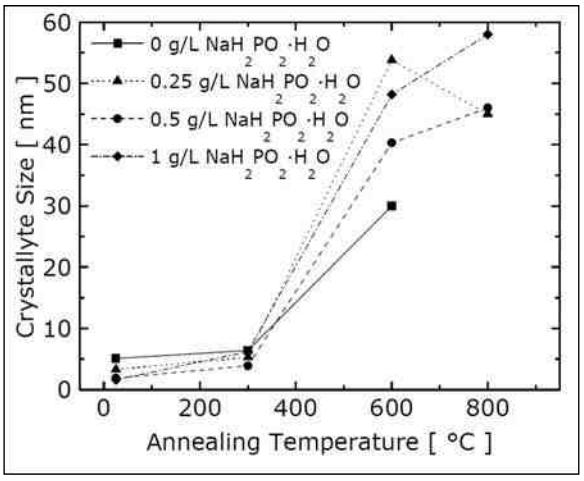

Figure 7—*Effect of annealing on the average size of crystallites.*

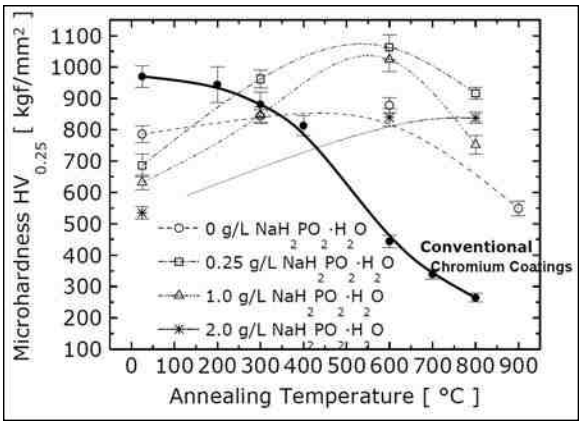

Figure 8—*Effect of annealing on microhardness of Ni-W-P coatings.*

Figure 8 also shows that hardness decreased with increasing phosphorus content for heat-treated and as-deposited coatings. This is attributable to the decrease in crystallization with increasing phosphorus content, which can be clearly observed in the XRD patterns of Ni-W-P (Fig. 7). This effect may be attributed to the fact that phosphorus was increasing the crystallization temperature of the material, as reported for other systems.[13]

Conclusions

In this work we studied the physicochemical and mechanical properties of Ni-W-P coatings electrodeposited onto steel by pulsed current as a function of phosphorus content and annealing temperatures. Specifically the main conclusions extracted from this study can be summarized as follow:

1. The addition of sodium hypophosphite to the Ni-W electroplating bath led to co-deposition of Ni-W-P. Increasing its concentration increased the amount of phosphorus in the coatings.

2. Microhardness values of the as-deposited Ni-W-P coatings were lower than those of corresponding Ni-W coatings.

3. Annealing caused the Ni-W-P coatings to reach hardness values (up to ~1050 kgf/mm^2) greater than those reached by as-deposited and annealed Ni-W coatings. This is attributed to the formation of Ni_3P within grain boundaries of the Ni-W matrix.

4. Increasing phosphorus content decreased the hardness of the annealed coatings. We attribute this to the fact that phosphorus increased the crystallization temperature of the materials.

References

1. B. Li, A. Lin & F. Gan, *Surface and Coatings Technology,* **201** (6), 2578 (2006).
2. G.J. Sargent, *Trans. Am. Electrochem. Soc.*, **37**, 479 (1920).
3. C.G. Fink, U.S. Patent 1,581,188 (1926).
4. J.P. Hoare, *J. Electrochem. Soc.*, **126** (2), 190 (1979).
5. G.A. Lausmann, *Surface and Coatings Technology*, **86-87** (2), 814 (1996).
6. I. Shuker & K.R. Newby, *Trans. Inst. Metal Fin.*, **83** (6), 272 (2005).
7. E.W. Brooman, *Proc. AESF SUR/FIN 2005*, NASF, Washington, DC, 2005; p. 164.
8. W-S. Hwang & J-J. Lee, *Materials Science Forum*, **510-511**, 1126 (2006).
9. N. Eliaz, T.M. Sridhar, & E. Gileadi, *Electrochimica Acta*, **50** (14), 2893 (2005).
10. S-K. Tien, J-G. Duh & Y-I. Chen, *Surface and Coatings Technology*, **177-178**, 532 (2004).
11. C.N. Panagopoulos, *et al.*, *Scripta Materialia*, **43** (7), 677 (2000).
12. V.D. Papacrhistos, *et al.*, *Materials Science and Engineering A*, **279** (1-2), 217 (2000).
13. M.J.L. Gines, F.J. Williams & C.A. Schuh, *Metallurgical and Materials Transactions A*, **38** (6), 1367 (2007).
14. A.J. Detor & C.A. Schuh, U.S. Patent Application 20060272949 (2006).
15. A.J. Detor & C.A. Schuh, *Acta Materialia*, **55** (1), 371 (2007).
16. H.P. Klug & L.E. Alexander, *X-ray Diffraction Procedures for Polycrystalline and Amorphous Materials*, 2nd Ed., John Wiley & Sons, New York, NY, 1974.
17. Z. Zhang, F. Zhou & E.J. Lavernia, *Metallurgical and Materials Transactions A*, **34** (6), 1349 (2003).
18. J. Ahmad, *et al.*, *Materials Transactions*, **44** (4), 705 (2003) (Japan Institute of Metals).
19. T. Yamasaki, *et al.*, *Nanostructured Materials,* **10** (3), 375 (1998).
20. T. Yamasaki, *et al.*, *Plating & Surface Finishing*, **87** (5), 148 (2000).
21. T. Yamasaki, *Mater. Phys. Mech.*, **1**, 127-132, (2000); http://www.ipme.ru/e-journals/MPM/no_2100/yamasaki/yamasaki.pdf
22. C.A. Schuh, T.G. Nieh & H.Iwasaki, *Acta Materialia*, **51** (2), 431 (2003).
23. S.C. Tjong & H. Chen, *Materials Science and Engineering R: Reports*, **45** (1-2), 1 (2004).

About the authors

Marcelo Gines

Jimena Loureiro

Federico Williams

Dr. Marcelo Gines is a senior researcher in the Surface Chemistry and Coating Department at the Center of Industrial Research of Tenaris (CINI-TENARIS). He received his M.S. in Chemical Engineering and his Ph.D. in Chemical Engineering from the Universidad Nacional del Litoral (UNL), Santa Fe, Argentina. He was a post doctoral research associate in the Department of Chemical Engineering, University of California at Berkeley. He is now a visiting researcher in the Department of Material Science and Engineering at Massachusetts Institute of Technology (MIT). His first research involved heterogeneous catalysis and he is now working on several chemical and electrochemical processes including electrodeposition of nanostructured alloys and composite materials, surface treatments and organic and metallic coatings involved in the steel industry. He has published more than fifteen papers in the field of chemical engineering.

Ms. Jimena Loureiro is an undergraduate Nanotechnology Engineering student at the University of Waterloo, Ontario, Canada. She has been part of a number of research groups including Surface and Coating Department at the Research and Development Center of Tenaris (REDE-AR-TENARIS), Polymer Research Group in the Chemical Engineering Department of the University of Waterloo, and Material Synthesis and Characterization Department at Xerox Research Centre of Canada (XRCC).

Dr. Federico Williams is Head of the Surface Chemistry and Coatings Department at the Centre of Industrial Research of Tenaris (CINI-TENARIS), and a Fellow of the Argentine National Council of Scientific Research (CONICET). He is also a Lecturer in Surface Chemistry at the University of Buenos Aires. He holds a Ph.D. in Physical Chemistry from the University of Cambridge (UK). His research is focused on endowing surfaces with new properties by using nanoparticles. Projects include self-cleaning surfaces, nanostructured surfaces, layer-by-layer self assembled monolayers, smart coatings and electrodeposition of nanostructured alloys and composite materials.